Вісник Тернопільського національного технічного університету
https://doi.org/10.33108/visnyk_tntu
Scientific Journal of the Ternopil National Technical University
2023, № 4 (112) https://doi.org/10.33108/visnyk_tntu2023.04
ISSN 2522-4433. Web: visnyk.tntu.edu.ua

UDC 539.3

SIMULATION OF A PRE-DEFORMED PLATE COMPRESSION BY TWO INDENTERS OF COMPLEX SHAPE

Hryhorii Habrusiev; Iryna Habrusieva; Borys Shelestovskyi

Ternopil Ivan Puluj National Technical University, Ternopil, Ukraine

Summary. *Within the framework of linearized formulation of the elasticity theory problems, the stress-strain state of a pre-deformed plate, which is modeled by a pre-stressed layer, is analyzed in the case of its smooth contact interaction with a two rigid axisymmetric indenters. The dual integral equations of the problem are solved by representing the quested-for functions in the form of a partial series sum by the Bessel functions with unknown coefficients. Finite systems of linear algebraic equations are obtained for determination of these coefficients. The influence of the initial strains on the magnitude and features of the contact stresses and vertical displacements on the surface of the plate is analyzed for the case of compressible and incompressible solids. In order to illustrate the results, the cases of the Bartenev – Khazanovich and the harmonic-type potentials are addressed.*

Key words: *pre-deformed plate, pre-stressed layer, contact stresses, vertical displacements, complex form indenter, dual integral equations.*

https://doi.org/10.33108/visnyk_tntu2023.04.091 *Received 07.09.2023*

Introduction. The calculation of the strength of structural elements and machine parts is one of the most important design stages. To minimize calculation errors, you need to take into account the maximum number of factors that affect the contact interaction of bodies. Therefore, it is imperative to take into account the presence of initial stresses and strains in the contacting bodies, as they can play a crucial role. In general, solving problems of this type requires the nonlinear theory of elasticity. However, for sufficiently high levels of initial deformations, a linearized formulation of the elasticity theory can be used. Scientists take such steps when solving problems in a variety of fields. In particular, the linearized formulation was used [1] to build a three-dimensional finite element model aimed at studying microdeformations in joints reinforced with isotropic and anisotropic fibers; to build a mathematical model aimed at studying the effect of initial stresses on wave propagation in a hollow infinite multilayer composite cylinder [2]. The geometrically linearized theory for incompressible materials was derived [3] from the nonlinear theory of elasticity in the small displacement regime. Using similar approaches [4], the asymptotic theory of beams for non-classical elastic materials was developed. The stress-strain state of a prestressed thick plate under the condition of its smooth contact interaction with a rigid axisymmetric annular indenter was also investigated using a linearized formulation of the problems of elasticity theory [5, 6].

It should be noted that the interaction of complex-shaped indentors with pre-stressed bodies has not yet been sufficiently studied. This paper demonstrates a methodology for determining the axisymmetric stress-strain state of a pre-stressed body using a plate as an example during its compression by two rigid indenters. The paper also investigates the effect of plate thickness and initial deformations on the distribution of contact stresses and vertical displacements of the plate surface.

Setting of the problem. Let us consider the axisymmetric problem of compression of a prestressed plate of thickness by two coaxial rigid parabolic indenters.

Corresponding author: Hryhorii Habrusiev; e-mail: habrusiev@gmail.com ……

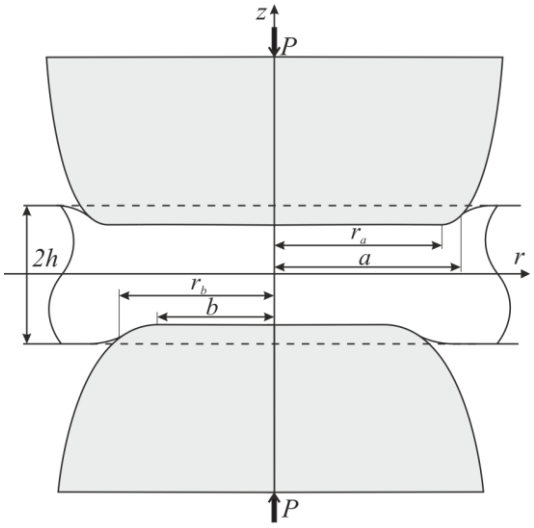

Figure 1. Diagram of contact interaction

We will model the plate as a prestressed isotropic layer [5,6]. Indentors are pressed into the layer progressively without rotation and friction under the action of a constant force P. Each indenter is formed by rotating a parabolic branch and a line segment perpendicular to the parabolic axis around a common axis. The focal parameters of the parabolas for the upper and lower indentors are respectively equal to R_1 and R_2. The axes of the parabolas bounding the indenters are parallel to the common axis of rotation, which coincides with the line of action of the forces P. Let's choose a cylindrical coordinate system (O, r, θ, z) so that the coordinate plane (O, r, θ) coincides with the median plane of the layer, and the axis Oz coincides with the axis of symmetry of the indenters (Fig. 1). The boundary conditions of the problem will be as follows:

$$\sigma_{zz}(r,h)=0,\ a\le r; \tag{1}$$

$$\sigma_{rz}(r,h)=0,\ 0\le r<\infty; \tag{2}$$

$$u_z(r,h)=\omega_1(r),\ 0\le r\le a; \tag{3}$$

$$\sigma_{zz}(r,-h)=0,\ b\le r; \tag{4}$$

$$\sigma_{rz}(r,-h)=0,\ 0\le r<\infty; \tag{5}$$

$$u_z(r,-h)=\omega_2(r),\ 0\le r\le b. \tag{6}$$

Functions $\omega_1(r)$ and $\omega_2(r)$ describe the shape of indentors. Let's choose them in the form of

$$\omega_1(r)=\begin{cases}\omega_1(a)-\dfrac{1}{2R_1}(a-r_a)^2,\ 0\le r<r_a;\\ \omega_1(a)+\dfrac{1}{2R_1}\left[(r-r_a)^2-(a-r_a)^2\right],\ r_a\le r\le a;\end{cases} \tag{7}$$

$$\omega_2(r)=\begin{cases}\omega_2(b)+\dfrac{1}{2R_2}(b-r_b)^2,\ 0\le r<r_b;\\ \omega_2(b)+\dfrac{1}{2R_2}\left[(b-r_b)^2-(r-r_b)^2\right],\ r_b\le r\le b.\end{cases} \tag{8}$$

where R_1 and R_2 are the focal parameters of the parabolas, which bound the upper and lower indenters, respectively.

Solution of the problem. We will assume that the residual stresses present in the layer to be homogeneous, so the following expressions for the components of the stress tensor and the displacement vector can be used to describe the stress-strain state of the layer [7]

$$\sigma_{rz}(r,z)=Q'_{3r}(r,z)=-c_{31}\int_0^\infty \alpha^3\left\{A_1 sh(\alpha z)+A_2\left[s_0 sh(\alpha z)+\alpha z ch(\alpha z)\right]+\right.$$
$$\left.+B_1 ch(\alpha z)+B_2\left[s_0\cdot ch(\alpha z)+\alpha z sh(\alpha z)\right]\right\}J_1(\alpha r)\,d\alpha;$$
$$\sigma_{zz}(r,z)=Q'_{33}(r,z)=c_{33}\int_0^\infty \alpha^3\left\{A_1 ch(\alpha z)+A_2\left[sch(\alpha z)+\alpha z sh(\alpha z)\right]+\right.$$
$$\left.+B_1 sh(\alpha z)+B_2\left[ssh(\alpha z)+\alpha z ch(\alpha z)\right]\right\}J_0(\alpha r)\,d\alpha;$$
$$u_r(r,z)=-\int_0^\infty \alpha^2\left\{A_1 ch(\alpha z)+A_2\left[ch(\alpha z)+\alpha z\, sh(\alpha z)\right]+\right.$$
$$\left.+B_1 sh(\alpha z)+B_2\left[sh(\alpha z)+\alpha z\, ch(\alpha z)\right]\right\}J_1(\alpha r)\,d\alpha;$$
$$u_z(r,z)=u_3(r,z)=m\int_0^\infty \alpha^2\left\{A_1 sh(\alpha z)+A_2\left[s_1 sh(\alpha z)+\alpha z\, ch(\alpha z)\right]+\right.$$
$$\left.+B_1 ch(\alpha z)+B_2\left[s_1 ch(\alpha z)+\alpha z\, sh(\alpha z)\right]\right\}J_0(\alpha r)\,d\alpha.$$

Having met the boundary conditions (1) and (2) on the upper boundary plane of the layer, at $z=h$, we derive:

$$\left.+B_1 sh(\alpha h)+B_2\left[s\, sh(\alpha h)+\alpha h\, ch(\alpha h)\right]\right\}J_0(\alpha r)\,d\alpha=0,\ a\le r<\infty; \tag{9}$$

$$-c_{31}\int_0^\infty \alpha^3\left\{A_1 sh(\alpha h)+A_2\left[s_0\, sh(\alpha h)+\alpha h\, ch(\alpha h)\right]+\right.$$
$$\left.+B_1 ch(\alpha h)+B_2\left[s_0\, ch(\alpha h)+\alpha h\, sh(\alpha h)\right]\right\}J_1(\alpha r)\,d\alpha=0,\ 0\le r<\infty; \tag{10}$$

$$m\int_0^\infty \alpha^2\left\{A_1 sh(\alpha h)+A_2\left[s_1\, sh(\alpha h)+\alpha h\, ch(\alpha h)\right]+\right.$$
$$\left.+B_1 ch(\alpha h)+B_2\left[s_1 ch(\alpha h)+\alpha h\, sh(\alpha h)\right]\right\}J_0(\alpha r)\,d\alpha=\omega_1(r),\ 0\le r\le a. \tag{11}$$

Similarly to (4) and (5), on the lower boundary plane of the layer, at $z=-h$, we obtain:

$$c_{33}\int_0^\infty \alpha^3\left\{A_1 ch(\alpha h)+A_2\left[s\, ch(\alpha h)+\alpha h\, sh(\alpha h)\right]-\right.$$
$$\left.-B_1 sh(\alpha h)-B_2\left[s\, sh(\alpha h)+\alpha h\, ch(\alpha h)\right]\right\}J_0(\alpha r)\,d\alpha=0,\ a\le r<\infty; \tag{12}$$

$$-c_{31}\int_0^\infty \alpha^3 \left\{-A_1 sh(\alpha h)-A_2\left[s_0\, sh(\alpha h)+\alpha h\, ch(\alpha h)\right]+\right.$$
$$\left.+B_1 ch(\alpha h)+B_2\left[s_0\, ch(\alpha h)+\alpha h\, sh(\alpha h)\right]\right\} J_1(\alpha r)\, d\alpha = 0,\ 0 \le r < \infty; \tag{13}$$

$$m\int_0^\infty \alpha^2 \left\{-A_1 sh(\alpha h)-A_2\left[s_1\, sh(\alpha h)+\alpha h\, ch(\alpha h)\right]+\right.$$
$$\left.+B_1 ch(\alpha h)+B_2\left[s_1 ch(\alpha h)+\alpha h\, sh(\alpha h)\right]\right\} J_0(\alpha r)\, d\alpha = \omega_2(r),\ 0 \le r \le b. \tag{14}$$

By applying the inverse formula of the Hankel integral transformation to relations (10) and (13), we obtain expressions for A_1, B_1 through A_2, B_2

$$A_1 = \frac{-1}{sh(\alpha h)}\left[s_0\, sh(\alpha h)+\alpha h\, ch(\alpha h)\right]A_2;$$

$$B_1 = \frac{-1}{ch(\alpha h)}\left[s_0\, ch(\alpha h)+\alpha h\, sh(\alpha h)\right]B_2. \tag{15}$$

By introducing two unknown functions $x(r)$ and $y(r)$, defined on the segments $[0,a]$ and $[0,b]$ respectively, we extend relations (9) and (12) to the entire positive semi-axis $[0,\infty)$

$$c_{33}\int_0^\infty \alpha^3 \left\{A_1\, ch(\alpha h)+A_2\left[s\, ch(\alpha h)+\alpha h\, sh(\alpha h)\right]+\right.$$
$$\left.+B_1\, sh(\alpha h)+B_2\left[s\, sh(\alpha h)+\alpha h\, ch(\alpha h)\right]\right\} J_0(\alpha r)\, d\alpha =$$
$$= x(r)\eta(a-r),\ \ 0 \le r < \infty; \tag{16}$$

$$c_{33}\int_0^\infty \alpha^3 \left\{A_1\, ch(\alpha h)+A_2\left[s\, ch(\alpha h)+\alpha h\, sh(\alpha h)\right]-\right.$$
$$\left.-B_1\, sh(\alpha h)-B_2\left[s\, sh(\alpha h)+\alpha h\, ch(\alpha h)\right]\right\} J_0(\alpha r)\, d\alpha =$$
$$= y(r)\eta(b-r),\ \ 0 \le r < \infty. \tag{17}$$

By applying the inverse formula of the Hankel integral transformation to equations (16) and (17), using the relations (15), we obtain a system of relatively unknowns A_2, B_2. Solving it, we will obtain

$$\alpha^2 A_2 = \frac{sh(\alpha h)}{2c_{33}\left[(s-s_0)\, ch(\alpha h)\, sh(\alpha h)-\alpha h\right]}\left[I_1(\alpha)+I_2(\alpha)\right];$$

$$\alpha^2 B_2 = \frac{ch(\alpha h)}{2c_{33}\left[(s-s_0)ch(\alpha h)sh(\alpha h)+\alpha h\right]}\left[I_1(\alpha)-I_2(\alpha)\right], \tag{18}$$

where

$$I_1(\alpha)=\int_0^a rx(r)J_0(r\alpha)dr;\ I_2(\alpha)=\int_0^b ry(r)J_0(r\alpha)dr.$$

Substituting expressions (7), (8), (15), (18) into relations (11) and (14), we will obtain:

$$\frac{k_1}{2}\int_0^\infty\left[\varphi_1(\alpha)I_1(\alpha)+\varphi_2(\alpha)I_2(\alpha)\right]\left(J_0(\alpha r)-J_0(\alpha a)\right)d\alpha = -\frac{1}{2R_1}(a-r_a)^2\eta(a-r)+ \\ +\frac{1}{2R_1}\left[(r-r_a)^2-(a-r_a)^2\right]\left\{\eta(r-r_a)-\eta(r-a)\right\}; \tag{19}$$

$$\frac{k_1}{2}\int_0^\infty\left[\psi_1(\alpha)I_1(\alpha)+\psi_2(\alpha)I_2(\alpha)\right]\left(J_0(\alpha r)-J_0(\alpha b)\right)d\alpha = \frac{1}{2R_2}(b-r_b)^2\eta(b-r)+ \\ +\frac{1}{2R_2}\left[(b-r_b)^2-(r-r_b)^2\right]\left\{\eta(r-r_b)-\eta(r-b)\right\}. \tag{20}$$

The following notations are used in the last equations:

$$\varphi_1(\alpha)=\Delta_1(\alpha)+\Delta_2(\alpha),\ \varphi_2(\alpha)=\Delta_1(\alpha)-\Delta_2(\alpha);$$

$$\psi_1(\alpha)=-\varphi_2(\alpha),\ \psi_2(\alpha)=-\varphi_1(\alpha);$$

$$\Delta_1(\alpha)=\frac{(s-s_0)sh^2(\alpha h)}{(s-s_0)ch(\alpha h)sh(\alpha h)-\alpha h},\ \Delta_2(\alpha)=\frac{(s-s_0)ch^2(\alpha h)}{(s-s_0)ch(\alpha h)sh(\alpha h)+\alpha h};$$

$$k_1=\frac{m(s_1-s_0)}{c_{33}(s-s_0)}=\frac{m_1(s_1-s_0)}{c_{44}(s-s_0)(1+m_1)l_1\sqrt{n_1}}.$$

The unknown functions $x(r)$ and $y(r)$ determine the distribution of contact stresses under the indentations. aking into account their continuity, as well as the absence of the contact area at the boundary (at $r=a$ and $r=b$), we represent $x(r)$ and $y(r)$ as a segment of the generalized Fourier series by the Bessel functions

$$x(r)=\sum_{n=1}^{N}a_nJ_0\left(\frac{r}{a}\beta_n\right),\ 0\le r\le a;$$

$$y(r)=\sum_{n=1}^{N}b_nJ_0\left(\frac{r}{b}\beta_n\right),\ 0\le r\le b, \tag{21}$$

where β_n – positive roots of the level $J_0(x)=0$.

Substituting the relation (21) into equations (19) and (20), we will obtain

$$\begin{aligned}&\frac{k_1}{2}\left\{\sum_{n=1}^{N}a_n\int_0^{\infty}\left[\varphi_1(\alpha)I_n^{(1)}(\alpha)\left(J_0(\alpha r)-J_0(\alpha a)\right)d\alpha+\right.\right.\\&\left.\left.+\sum_{n=1}^{N}b_n\int_0^{\infty}\left[\varphi_2(\alpha)I_n^{(2)}(\alpha)\left(J_0(\alpha r)-J_0(\alpha a)\right)d\alpha\right\}=\right.\\&=\frac{1}{2R_1}\left(r-r_a\right)^2\eta\left(r-r_a\right)-\frac{1}{2R_1}\left(a-r_a\right)^2,\ 0\le r\le a;\end{aligned}\tag{22}$$

$$\begin{aligned}&\frac{k_1}{2}\left\{\sum_{n=1}^{N}a_n\int_0^{\infty}\left[\psi_1(\alpha)I_n^{(1)}(\alpha)\left(J_0(\alpha r)-J_0(\alpha b)\right)d\alpha+\right.\right.\\&\left.\left.+\sum_{n=1}^{N}b_n\int_0^{\infty}\left[\psi_2(\alpha)I_n^{(2)}(\alpha)\left(J_0(\alpha r)-J_0(\alpha b)\right)d\alpha\right\}=\right.\\&=-\frac{1}{2R_2}\left(r-r_b\right)^2\eta\left(r-r_b\right)+\frac{1}{2R_2}\left(b-r_b\right)^2,\ 0\le r\le b;\end{aligned}\tag{23}$$

$$I_n^{(1)}(\alpha)=\int_0^a rJ_0\left(\frac{r}{a}\beta_n\right)J_0(r\alpha)dr;\quad I_n^{(2)}(\alpha)=\int_0^b rJ_0\left(\frac{r}{b}\beta_n\right)J_0(r\alpha)dr.$$

Multiplying relations (22) and (23) by $rJ_0\left(\frac{r}{a}\beta_q\right)$ та $rJ_0\left(\frac{r}{b}\beta_q\right)$, $q=\overline{1,N}$, respectively, and integrating the obtained expressions r from 0 to a and from 0 to b, we will obtain

$$\begin{aligned}&\sum_{n=1}^{N}a_nK_{qn}^{(11)}(\alpha)+\sum_{n=1}^{N}b_nK_{qn}^{(12)}(\alpha)=B_q^{(1)};\\&\sum_{n=1}^{N}a_nK_{qn}^{(21)}(\alpha)+\sum_{n=1}^{N}b_nK_{qn}^{(22)}(\alpha)=B_q^{(2)};\end{aligned}\tag{24}$$

$$K_{qn}^{(11)}(\alpha)=\int_0^{\infty}\left[\varphi_1(\alpha)I_n^{(1)}(\alpha)\left[I_q^{(1)}(\alpha)-J_0(a\alpha)F_q^{(1)}\right]d\alpha;\right.$$

$$K_{qn}^{(12)}(\alpha)=\int_0^{\infty}\left[\varphi_2(\alpha)I_n^{(2)}(\alpha)\left[I_q^{(1)}(\alpha)-J_0(a\alpha)F_q^{(1)}\right]d\alpha;\right.$$

$$K_{qn}^{(21)}(\alpha)=\int_0^{\infty}\left[\psi_1(\alpha)I_n^{(1)}(\alpha)\left[I_q^{(2)}(\alpha)-J_0(b\alpha)F_q^{(2)}\right]d\alpha;\right.$$

$$K_{qn}^{(22)}(\alpha)=\int_0^{\infty}\left[\psi_2(\alpha)I_n^{(2)}(\alpha)\left[I_q^{(2)}(\alpha)-J_0(b\alpha)F_q^{(2)}\right]d\alpha;\right.$$

$$B_q^{(1)} = \frac{1}{k_1 R_1}\left[\int_{r_a}^{a} r\left(r-r_a\right)^2 J_0\left(\frac{r}{a}\beta_q\right)dr - \left(a-r_a\right)^2 \int_0^a r J_0\left(\frac{r}{a}\beta_q\right)dr\right];$$

$$B_q^{(2)} = \frac{1}{k_1 R_2}\left[\left(b-r_b\right)^2 \int_0^b r J_0\left(\frac{r}{b}\beta_q\right)dr - \int_{r_b}^{b} r\left(r-r_b\right)^2 J_0\left(\frac{r}{b}\beta_q\right)dr\right];$$

$$F_q^{(1)} = \int_0^a r J_0\left(\frac{r}{a}\beta_q\right)dr; \quad F_q^{(2)} = \int_0^b r J_0\left(\frac{r}{b}\beta_q\right)dr.$$

Using the superposition method and entering the notation

$$a_n = \frac{1}{k_1}\left[\frac{1}{R_1}a_n^{(1)} + \frac{1}{R_2}a_n^{(2)}\right],\ b_n = \frac{1}{k_1}\left[\frac{1}{R_1}b_n^{(1)} + \frac{1}{R_2}b_n^{(2)}\right], \tag{25}$$

from (24) we obtain the systems of equations for the unknowns $a_n^{(1)}$, $a_n^{(2)}$, $b_n^{(1)}$ and $b_n^{(2)}$, $n=\overline{1,N}$.

The values R_1 and R_2 in the relations (25) determine from the conditions of equilibrium

$$2\pi\int_0^a r\sigma_{zz}\left(r,h\right)dr = -P; \qquad 2\pi\int_0^b r\sigma_{zz}\left(r,-h\right)dr = -P. \tag{26}$$

Taking into account (26) from inequalities (21), (25), we obtain the system with respect to

$$R^{(1)} \text{ та } R^{(2)}$$

$$\begin{cases} R^{(1)}\sum_{n=1}^{N} a_n^{(1)} F_q^{(1)} + R^{(2)}\sum_{n=1}^{N} a_n^{(2)} F_q^{(1)} = -1; \\ R^{(1)}\sum_{n=1}^{N} b_n^{(1)} F_n^{(2)} + R^{(2)}\sum_{n=1}^{N} b_n^{(2)} F_q^{(2)} = -1; \end{cases} \tag{27}$$

$$R^{(i)} = \frac{1}{k_1 R_i}\frac{2\pi}{P}, \quad i=1,2.$$

Having solved system (27), from relations (21) and (25), we obtain the formulas for finding the function of contact stress distribution under indenters

$$\begin{aligned} \sigma_{zz}\left(r,h\right) &= \frac{P}{2\pi}\sum_{n=1}^{N}\left[R^{(1)}a_n^{(1)} + R^{(2)}a_n^{(2)}\right]J_0\left(\frac{r}{a}\beta_n\right), \\ \sigma_{zz}\left(r,-h\right) &= \frac{P}{2\pi}\sum_{n=1}^{N}\left[R^{(1)}b_n^{(1)} + R^{(2)}b_n^{(2)}\right]J_0\left(\frac{r}{b}\beta_n\right), \end{aligned} \tag{28}$$

as well as expressions for determining the vertical displacements of the points of the upper and lower planes of the layer

$$u_z(r,h)=\frac{k_1}{2}\frac{P}{2\pi}\left\{\sum_{n=1}^{N}\left(R^{(1)}a_n^{(1)}+R^{(2)}a_n^{(2)}\right)\int_0^{\infty}\varphi_1(\alpha)I_n^{(1)}(\alpha)J_0(\alpha r)d\alpha+\right.$$
$$\left.+\sum_{n=1}^{N}\left(R^{(1)}b_n^{(1)}+R^{(2)}b_n^{(2)}\right)\int_0^{\infty}\varphi_2(\alpha)I_n^{(2)}(\alpha)J_0(\alpha r)d\alpha\right\}; \quad (29)$$

$$u_z(r,-h)=\frac{k_1}{2}\frac{P}{2\pi}\left\{\sum_{n=1}^{N}\left(R^{(1)}a_n^{(1)}+R^{(2)}a_n^{(2)}\right)\int_0^{\infty}\psi_1(\alpha)I_n^{(1)}(\alpha)J_0(\alpha r)d\alpha+\right.$$
$$\left.+\sum_{n=1}^{N}\left(R^{(1)}b_n^{(1)}+R^{(2)}b_n^{(2)}\right)\int_0^{\infty}\psi_2(\alpha)I_n^{(2)}(\alpha)J_0(\alpha r)d\alpha\right\}.$$

Numerical example. Let us investigate the effect of the layer thickness and the residual deformation field on the distribution of contact stresses and vertical displacements of the points of the layer boundary planes.

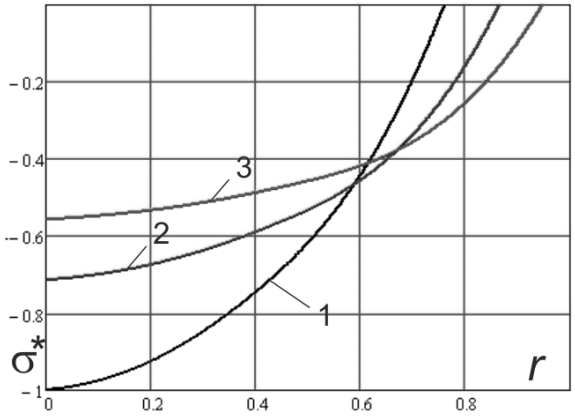

Figure 2. Contact stresses

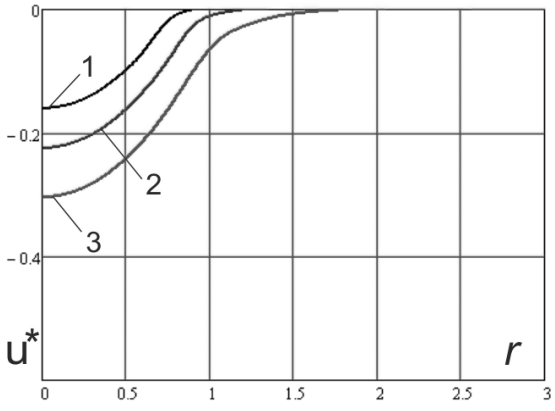

Figure 3. Vertical displacements

Fig. 2 shows a graph of the function $\sigma^*(r)$, describing the distribution of contact stresses for the case of compression of the layer by two identical co-axial parabolic indenters at $R_1=R_2=2$, $r_a=r_b=0$. The graph of the value of $u^*(r)$, describing the vertical displacements of the points of the boundary planes of the layer for the same case, is shown in Fig. 3. Curve 1 corresponds to the layer thickness $H=0.5$, curve 2 – $H=1$, curve 3 – $H=2$. As can be seen from the figures, the layer thickness affects the extreme values of contact stresses. In particular, when the layer is compressed with thickness $H=0.5$ the extreme values of contact stresses are 40% higher than at $H=1$.

The coefficient k_1, which is determined by the ratio

$$k_1=\frac{m_1(s_1-s_0)}{c_{44}(1+m_1)(s-s_0)l_1\sqrt{n_1}},$$

characterises the effect of initial deformations and depends on the structure of the elastic potential of the prestressed plate. In particular, in the case of the Bartenev-Khazanovich potential

$$k_1 = \frac{2(1+\nu)}{E} \frac{\lambda_1^{\frac{7}{2}}}{3\lambda_1^3 - 1},$$

where ν – Poisson's ratio, E – Young's modulus of the plate material. The latter ratio tends to infinity at $3\lambda_1^3 - 1 = 0$, i.e. at $\lambda_1 \to \lambda_{kp} \approx 0.693$. The value λ_{kp} corresponds to surface instability under uniform biaxial compression. In this case, the vertical displacements of the boundary plane points increase unlimitedly, and there are no contact stresses. Thus, the following mechanical effect is observed: when λ_1 is approaching the critical value λ_{kp} the phenomena of «resonant nature» occur in the plate, which were previously discovered by O.M. Guz in the problems of brittle fracture of materials with initial stresses [7]. A similar effect is observed in bodies with an elastic potential of harmonic type. The coefficient k_1 in this case takes the form

$$k_1 = \frac{2(1-\nu^2)}{E} \frac{\lambda_1^2}{\lambda_1(2+\nu) - (1+\nu)}.$$

For different materials, the critical values λ_{kp} are different because they depend on ν. In particular, at $\nu = 0.3$ «resonance» phenomena are observed at $\lambda_1 \to \lambda_{kp} \approx 0.565$. Figure 4 illustrates the dependence of the coefficient k_1 on λ_1 for the case of the Bartenev-Khazanovich potential (curve 1) and the harmonic potential (curve 2).

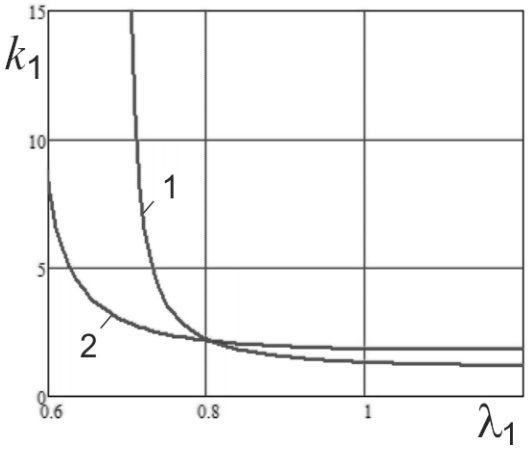

Figure 4. Dependence of k_1 and on λ_1

Conclusions. Regardless of the shape of the indenter and the presence of residual deformations, the distribution of contact stresses for a layer with a thickness of at least twice the radius of the contact area is similar to the corresponding distribution for a half-space.

The presence of residual tensile deformations in the layer causes a narrowing of the contact area, an increase in the absolute value of contact forces and a decrease in vertical displacements. The magnitude of the induced changes depends on the type of elastic potential. The presence of residual compressive deformations in the layer, in turn, causes the expansion of the contact area, a decrease in the absolute value of contact stresses and an increase in vertical displacements.

References

1. Lapusta Y., Harich J., Wagner W. Three-dimensional FE model for fiber interaction effects during microbuckling in composites with isotropic and anisotropic fibers. Commun. Numer. Meth. Eng. 2008. 24, No. 12. P. 2206–2215. https://doi.org/10.1002/cnm.1084
2. Mahesh S., Selvamani R. and Ebrahami F. Assessment of hydrostatic stress and thermo piezoelectrici-ty in a laminated multilayered rotating hollow cylinder. Mechanics of Advanced Composite Structures. 2021. Volume 8. Issue 1. P. 77–86.
3. Jesenko M., Schmidt B. Geometric linearization of theories for incompressible elastic materials and applications. Mathematical Models and Methods in Applied Sciences. 2021. Volume 31. Issue 4. P. 829–860. https://doi.org/10.1142/S0218202521500202
4. Diandian Gu, Chenbo Fu, Hui-Hui Dai, K.R. Rajagopal, Asymptotic beam theory for non-classical elastic materials. International Journal of Mechanical Sciences. Volume 189. 2021. 105950, ISSN 0020-7403, URL: https://doi.org/10.1016/j.ijmecsci.2020.105950. https://doi.org/10.1016/j.ijmecsci.2020.105950
5. Habrusiev H., Habrusieva I. (2021). Contact interaction of a predeformed plate which lies without friction on rigid base with a parabolic indenter. Scientific Journal of TNTU (Tern.). Vol. 102. P. 87–95. https://doi.org/10.33108/visnyk_tntu2021.02.087
6. Habrusiev H., Habrusieva I., Shelestovs'kyi B. (2018). The effect of initial deformations of the thick plate on its contact interaction with the ring punch. Scientific Journal of TNTU (Tern.). Vol. 90. No. 2. P. 50–59. https://doi.org/10.33108/visnyk_tntu2018.02.050
7. A. N. Guz' and V. B. Rudnitskii, Foundations of the Theory of Contact Interaction of Elastic Bodies with Initial (Residual) Stresses, PP Mel'nik, Khmel'nitskii (2006) P. 710. [In Russian].

Список використаних джерел

1. Lapusta Y., Lapusta Y., Wagner W. Three-dimensional FE model for fiber interaction effects during microbuckling in composites with isotropic and anisotropic fibers. Commun. Numer. Meth. Eng. 2008. 24. No. 12. P. 2206–2215. https://doi.org/10.1002/cnm.1084
2. Mahesh S., Selvamani R., Ebrahami F.Assessment of hydrostatic stress and thermo piezoelectrici-ty in a laminated multilayered rotating hollow cylinder. Mechanics of Advanced Composite Structures. 2021. Volume 8. Issue 1. P. 77–86.
3. Jesenko M., Schmidt B. Geometric linearization of theories for incompressible elastic materials and applications. Mathematical Models and Methods in Applied Sciences. 2021. Volume 31. Issue 4. P. 829–860. https://doi.org/10.1142/S0218202521500202
4. Diandian Gu, Chenbo Fu, Hui-Hui Dai, K.R. Rajagopal Asymptotic beam theory for non-classical elastic materials. International Journal of Mechanical Sciences. Volume 189. 2021. 105950, ISSN 0020-7403. URL: https://doi.org/10.1016/j.ijmecsci.2020.105950. https://doi.org/10.1016/j.ijmecsci.2020.105950
5. Habrusiev H., Habrusieva I. Contact interaction of a predeformed plate which lies without friction on rigid base with a parabolic indenter. Scientific Journal of TNTU. 2021. Vol. 102. P. 87–95. https://doi.org/10.33108/visnyk_tntu2021.02.087
6. Habrusiev H., Shelestovs'kyi B. The effect of initial deformations of the thick plate on its contact interaction with the ring punch. Scientific Journal of TNTU. 2018. Vol. 90. No. 2. P. 50–59. https://doi.org/10.33108/visnyk_tntu2018.02.050
7. Гузь А. Н., Рудницкий В. Б. Основы теории контактного взаимодействия упругих тел с начальными (остаточными) напряжениями. Хмельницкий: 2006, 710 с.

УДК 539.3

МОДЕЛЮВАННЯ СТИСНЕННЯ ПОПЕРЕДНЬО ДЕФОРМОВАНОЇ ПЛАСТИНИ ДВОМА ІНДЕНТОРАМИ СКЛАДНОЇ ФОРМИ

Григорій Габрусєв; Ірина Габрусєва; Борис Шелестовський

Тернопільський національний технічний університет імені Івана Пулюя, Тернопіль, Україна

Резюме. *Продемонстровано розроблену методику побудови розв'язків осесиметричних задач визначення напруженого стану заздалегідь деформованої пружної плити при її контактній взаємодії з двома жорсткими інденторами складної конфігурації. Співвідношення, що описують напружено-*

деформований стан тіл із початковими деформаціями, наведено у рамках лінеаризованої постановки задачі теорії пружності. Із використанням запропонованої методики досліджено напружено-деформований стан заздалегідь деформованої плити при її гладкому контакті з двома жорсткими осесиметричними параболічними інденторами складної конфігурації. Побудову аналітичних розв'язків контактної задачі для попередньо деформованої плити проведено шляхом її моделювання попередньо напруженим ізотропним шаром. Граничні умови в зоні контакту сформульовано в класичній постановці (відсутність дотичних напружень на граничній поверхні шару, відсутність нормальних напружень за межами зони контакту, вертикальність зміщення індентора). У результаті підстановки виразів для компонент напружено-деформованого стану плити в граничні умови побудовано систему двох парних інтегральних рівнянь, ядра яких містять функції Бесселя. Подаючи функцію розподілу контактних напружень під інденторами у вигляді скінченного ряду за функціями Бесселя. Задачу зведено до скінченої системи лінійних алгебраїчних рівнянь відносно невідомих коефіцієнтів ряду. Побудовано аналітичні вирази для контактних напружень та вертикальних переміщень межових точок плити. Застосувавши отримані співвідношення, проаналізовано вплив початкових деформацій на рівень та характер контактних напружень і вертикальних переміщень межової площини плити у випадках стисливого та нестисливого матеріалу. Числовий аналіз проведено для випадків наявності у плиті пружного потенціалу Бартенєва – Хазановича, а також потенціалу гармонічного типу.

Ключові слова: *попередньо деформована плита, попередньо напружений шар, контактні напруження, вертикальні переміщення, параболічний індентор, подвійні інтегральні рівняння.*

https://doi.org/10.33108/visnyk_tntu2023.04.091 *Отримано 07.09.2023*